

maximum intensity at 550 nm, a region where **1** does not absorb, and decays unimolecularly with $\tau = 300 \mu\text{s}$. The observed signal is assigned to $M_2 \rightarrow \mu\text{-LCT}$ triplet–triplet absorbance (vide infra). The transient absorbance exhibits partial saturation at high laser powers,^{18–20} suggesting that the observed state is formed by a process of limited efficiency from the initial excited state, consistent with $[M_2 \rightarrow \mu\text{-LCT}]^1 \rightarrow [M_2 \rightarrow \mu\text{-LCT}]^3$ conversion. The method of Carmichael and Hug¹⁹ was employed to fit the partial saturation of transient absorbance and obtain the triplet conversion quantum yield, $\Phi_T = 0.2$.

In the presence of CO_2 , the rate of disappearance of $[M_2 \rightarrow \mu\text{-LCT}]^3$ absorbance exhibits a first-order dependence on $[\text{CO}_2]$. The photochemical kinetics of **1** with CO_2 were examined over the CO_2 pressure range 1–3 atm. Pressures of CO_2 were calibrated against $[\text{CO}_2]$ in THF solution by the method of Daniele et al.²¹ The lifetime τ of $[M_2 \rightarrow \mu\text{-LCT}]^3$ absorbance exhibits an inverse linear dependence on $[\text{CO}_2]$ from which the rate constant for CO_2 addition, $k_{\text{CO}_2} = 1 \times 10^4 \text{ M}^{-1} \text{ s}^{-1}$, was determined. The $[M_2 \rightarrow \mu\text{-LCT}]^3$ state of **1** is also reactive with respect to the addition of a variety of other reagents. For example PhCl , which is thermally unreactive with **1** when employed as the solvent under reflux, reacts photochemically with the $[M_2 \rightarrow \mu\text{-LCT}]^3$ state with a bimolecular rate constant, $k_{\text{PhCl}} = 4 \times 10^3 \text{ M}^{-1} \text{ s}^{-1}$, to form the μ -phenyl amino-carbyne complex, $[\text{Ni}_2(\mu\text{-CN}(\text{Ph})\text{Me})(\text{CNMe})_2(\text{dppm})_2]\text{Cl}$, **3**.²² The dependence of $k_{\text{obsd}} = 1/\tau$ for the transient absorbance of **1** versus $[\text{CO}_2]$ and $[\text{PhCl}]$ is given in Figure 1. The overall photochemical reactivity of **1** with CO_2 and PhCl is presented in Scheme I.

The nature of the lowest energy electronic absorption spectral band of **1** was also assessed by bridging ligand substituent and solvent effects. The electronic absorption spectrum of **1** exhibits an intense, broad band centered at $\lambda_{\text{max}} = 345 \text{ nm}$ ($\epsilon = 19\,000 \text{ M}^{-1} \text{ cm}^{-1}$) in THF. The series of μ -aryl isocyanide complexes $\text{Ni}_2(\mu\text{-L})(\text{CNMe})_2(\text{dppm})_2$, $\text{L} = \text{CNC}_6\text{H}_6$ (**4**), $\text{CN-}p\text{-C}_6\text{H}_4\text{Cl}$ (**5**), and $\text{CN-}p\text{-C}_6\text{H}_4\text{Me}$ (**6**), were prepared by substitution of one of the MeNC ligands of **1**.²³ Within the group of complexes **4–6** values of λ_{max} are quite insensitive to the nature of the para substituent on the aryl group but are shifted to longer wavelengths by 35 nm relative to the μ -methyl isocyanide complex **1** in THF.²³ There are also significant intensity differences between the aryl complexes **4–6** and **1**. The values of ϵ determined for the aryl complexes **4–6** are 20–100% higher than the values for **1** in THF and benzene. The bathochromic shifts and intensity increases resulting from replacement of alkyl substituent with aryl substituents are consistent with metal-to- μ -ligand charge transfer ($M_2 \rightarrow \mu\text{-LCT}$).²⁴ The electronic absorption spectra of the μ -isocyanide complexes **1** and **4–6** also exhibit significant solvent dependence. Hypsochromic shifts as large as 85 nm (THF/MeCN) are observed in more polar solvents. This is consistent with a Frank–Condon destabilized excited state model in which a polar solvent is unable to reorient itself in response to an excited state of polarity markedly different from the ground state. Extended Huckel calculations support the notion of metal-to-bridging ligand charge transfer. In an electronically saturated $d^{10}\text{--}d^{10}$ configuration of nickel atoms interacting with unsaturated methyl isocyanide ligands, bridging isocyanide $\pi^*/\text{Ni}_2 d\pi^*$ interactions

determine both the HOMO and LUMO.²⁵ The $\pi^*(\parallel)$ component of the $\mu\text{-CNMe}$ ligand and highest energy $\text{Ni}_2 d\pi^*$ combination contribute to a HOMO of metal–ligand π -bonding character. The second π^* component (\perp) of the $\mu\text{-CNMe}$ ligand is not disposed by symmetry to interact significantly with the Ni_2 framework and becomes the LUMO. The Huckel description thus predicts a LUMO of essentially pure $\mu\text{-CNMe}$ π^* character, consistent with the spectroscopic studies described above.

Our results suggest that a long-lived excited state of a binuclear transition-metal complex can be employed to associate with the CO_2 molecule. Previous studies from this laboratory indicate that the association of CO_2 with **1** results in the activation of CO_2 toward oxygen atom transfer reactions.^{8,13} Continued studies of the photochemical activation and reduction of CO_2 are presently underway.

Acknowledgment. We are extremely grateful to Professor George McLendon (Rochester), Professors Dave McMillin and Ed Grant (Purdue), and Dr. Jay Winkler (Brookhaven) for suggestions and helpful discussions, Professor William Jorgensen (Purdue) for assistance and support with extended Huckel calculations, and NSF (CHE-8707963) for support.

Supplementary Material Available: Description and diagrammatic layout of laser flash photolysis system; preparative details, IR, UV–vis, and $^1\text{P}\{^1\text{H}\}$ NMR spectroscopic data for **4**, **5**, and **6**; transient absorbance versus laser power data; and details of the determination of triplet conversion quantum yield (5 pages). Ordering information is given on any current masthead page.

(25) All calculations were performed for $\text{Ni}_2(\mu\text{-CNH})(\text{CNH})_2\text{-}(\text{PH}_2\text{CH}_2\text{PH}_2)_2$ with the extended Huckel method. See: Hoffmann, R. J. *J. Chem. Phys.* **1963**, *39*, 1397. the parameters used for nickel were adopted in the present study from earlier work of Hoffmann, see: Hoffmann, D. M.; Hoffmann, R.; Fisel, C. R. *J. Am. Chem. Soc.* **1982**, *104*, 3858.

Transition-State Geometry in Epoxidation by Iron–Oxo Porphyrin at the Compound I Oxidation Level. Epoxidation of Alkenes Catalyzed by a Sterically Hindered (*meso*-Tetrakis(2,6-dibromophenyl)porphinato)iron(III) Chloride

Dražen Ostović and Thomas C. Bruice*

Department of Chemistry
University of California at Santa Barbara
Santa Barbara, California 93106

Received May 9, 1988

Although many studies of iron porphyrin catalyzed epoxidations have appeared in the literature,^{1–3} the mechanism of epoxidation remains unresolved. The following mechanisms have been considered: (i) concerted oxygen insertion into the double bond (the oxenoid character of the iron bound oxygen atom supports this

(18) Transient absorbance versus laser power data and details of the determination of the triplet conversion quantum yield, Φ_T , are included as Supplementary Material.

(19) (a) Carmichael, I.; Hug, G. L. *J. Phys. Chem.* **1985**, *89*, 4036. (b) Hug, G. L.; Carmichael, I. *J. Photochem.* **1985**, *31*, 179.

(20) Murasecco-Suardi, P.; Gassmann, E.; Braun, A. M.; Oliveros, E. *Helv. Chim. Acta* **1987**, *70*, 1760.

(21) Daniele, S.; Ugo, P.; Bontempelli, G.; Fiorani, M. *J. Electroanal. Chem.* **1987**, *219*, 259.

(22) Complex **3** was prepared by photolysis ($\lambda = 355$ or 366 nm) of a PhCl solution of **1** or, as the corresponding iodide salt, by addition of excess MeI ($3 \mu\text{L}$, 0.05 mmol) to a THF solution of **4** (0.026 g , 0.025 mmol). Recrystallization from THF/hexanes affords the crystalline solid, yield 90%. $[\text{Ni}_2(\mu\text{-CN}(\text{Ph})\text{Me})(\text{CNMe})_2(\text{dppm})_2]\text{Cl}$ (**3**): IR (KBr) ν (CN) 2135 s , 1523 m cm^{-1} ; $^1\text{P}\{^1\text{H}\}$ NMR δ 20.2 (m); UV–vis (λ_{max} (ϵ)) 550 nm (1600) (THF).

(23) Details of the preparation of complexes **4**, **5**, and **6** and their IR, UV–vis, and $^1\text{P}\{^1\text{H}\}$ data are included as Supplementary Material.

(24) Phifer, C. C.; McMillin, D. R. *Inorg. Chem.* **1986**, *25*, 1329.

(1) *Cytochrome P-450; Structure, Mechanism, and Biochemistry*; Ortiz de Montellano, P. R., Ed.; Plenum: New York, 1986.

(2) (a) Watabe, T.; Akamatsu, K. *Biochem. Pharmacol.* **1976**, *23*, 1079.

(b) Watabe, T.; Ueno, Y.; Imazumi, J. *Biochem. Pharmacol.* **1971**, *20*, 912.

(c) Ortiz de Montellano, P. R.; Mangold, B. L. K.; Wheeler, C.; Kunze, K. L.; Reich, N. O. *J. Biol. Chem.* **1983**, *258*, 4212. (d) Castellino, A. J.; Bruice, T. C. *J. Am. Chem. Soc.* **1988**, *110*, 1313.

(3) (a) Traylor, T. G.; Nakano, T.; Mikszal, A. R.; Dunlap, B. E. *J. Am. Chem. Soc.* **1987**, *109*, 3625. (b) Traylor, T. G.; Nakano, T.; Dunlap, B. E.; Traylor, P.; Dolphin, D. *J. Am. Chem. Soc.* **1986**, *108*, 2782. (c) Traylor, T. G.; Mikszal, A. R. *J. Am. Chem. Soc.* **1987**, *109*, 2770. (d) Castellino, A. J.; Bruice, T. C. *J. Am. Chem. Soc.* **1988**, *110*, 158. (e) Liebler, D. C.; Guengerich, F. P. *Biochemistry* **1983**, *22*, 5482. (f) Mansuy, D.; Leclaire, J.; Fontecave, M.; Momenteau, M. *Biochem. Biophys. Res. Commun.* **1984**, *119*, 319. (g) Groves, J. T.; Subramanian, D. V. *J. Am. Chem. Soc.* **1984**, *106*, 2177.

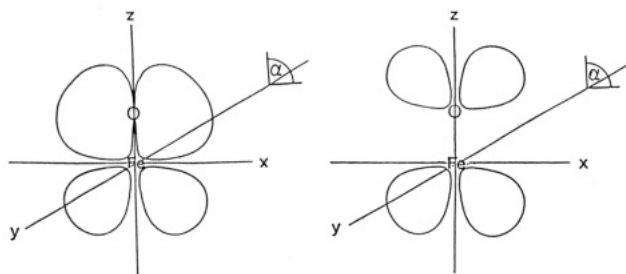
Table I. Epoxide Yields Using $(\text{Br}_8\text{TPP})\text{Fe}^{\text{III}}(\text{Cl})$ ($3.4\text{--}15 \times 10^{-5}$ mmol) and $\text{C}_6\text{F}_5\text{IO}$ ($2\text{--}20 \times 10^{-3}$ mmol) in Grade A CH_2Cl_2 (0.6–1.0 mL) at Room Temperature

alkene	alkene concntrtn (M)	catalyst turnover	epoxide yield ^a (%)
TME	1.0	200	99
	0.1	170	98
	0.01	200	92
	1.0		1 ^c
norbornene	1.0	250	99
	0.1	140	93
	0.01	100	82
	1.0		4 ^c
<i>cis</i> -stilbene ^d	0.25	125	99
	0.05	60	94
	0.025	45	93
	0.25		3 ^c
<i>trans</i> -stilbene	0.14	175	4
	0.025	170	4
	0.14		3 ^c

^aThe reaction times were dependent on the turnover number, typically about 10 min for 100 turnovers. ^bYields are based on oxidant. ^cCatalyst was not present in these runs. ^d<0.1% of *trans*-stilbene and 0.5–1.5% *trans*-epoxide were observed.

view⁴), (ii) initial e^- transfer from alkene π bond to the iron–oxo porphyrin,^{3a–c} or (iii) initial formation of an intermediate with Fe–O–C bonding (carbon radical, carbocation, or metallaoxetane), followed by collapse to the epoxide. Retention of stereochemistry is in accord with a concerted insertion of oxygen into the double bond,^{1,2} while porphyrin N-alkylation, substrate rearrangements, and $1e^-$ oxidizability of alkenes^{3c} have been offered to support nonconcerted epoxidation.^{1,3} It is not clear, however, whether the N-alkylation of the porphyrin and substrate rearrangements arise from intermediates along the reaction path to the epoxide or if $1e^-$ oxidation of alkene is on the epoxidation reaction path.

On the basis of the steric selectivity observed in the epoxidation of various alkenes by iron(IV)–oxo porphyrin π -cation radical $((^+\text{P})\text{Fe}^{\text{IV}}=\text{O})$, Groves proposed a mechanism in which alkene approaches the Fe–O bond from the side and parallel to the porphyrin ring.⁵ It is argued that the structure expected for Fe^{IV} in $((^+\text{P})\text{Fe}^{\text{IV}}=\text{O})$ complex will have two singly occupied d_{xz} and d_{yz} orbitals considerably mixed with the filled p-orbitals on the oxygen so that the iron bound oxygen atom possesses considerable unpaired electron density and an oxenoid character.^{4,6} However, the resulting Fe–O $d_{\pi}\text{--}p_{\pi}$ bonding and antibonding orbitals would not be parallel to the porphyrin ring as depicted by Groves.^{5,7} Considerable electron density on the side of oxygen distal to the porphyrin iron is expected in orbitals of this type I.⁸ Thus, alkene need not approach the Fe–O bond in a perpendicular fashion but rather with the moderate optimum angle α (I).



In order to test this theory we prepared (*meso*-tetrakis(2,6-dibromophenyl)porphyrinato)iron(III) chloride $((\text{Br}_8\text{TPP})\text{Fe}^{\text{III}}(\text{Cl}))$,⁹

Figure 1. Space-filling models (CPK) showing the docking of 2,3-dimethyl-2-butene (TME) to (*meso*-tetrakis(2,6-dibromophenyl)porphyrinato)iron(III) chloride. The energy of interaction is 0.6 kcal/mol. Graphics were obtained in the following manner. By using Polygen programs QUANTA and CHARMM, the structure of (*meso*-tetrakis(2,6-dibromophenyl)porphyrinato)iron(III) chloride¹⁴ with C–Br bond lengths kept at 1.85 Å. An Fe=O bond was created with the length of 1.64 Å (as in the compound I species¹⁵). To minimize the steric interaction of the bromine substituents with the pyrrole hydrogens of the porphyrin moiety, the torsion angles between the phenyl and porphyrin rings were energy minimized. The structure of TME is a CHARMM minimized structure. Inspection of view A shows that TME can be fit into the niche created by the bromo substituents. Inspection of view B and real time energy calculations show that TME can be docked on top of the oxygen atom to a minimum angle $\alpha = 40^\circ$ without serious interactions with *o*-bromines or porphyrin ring. Similar experiments were performed with norbornene and *cis*- and *trans*-stilbenes. The corresponding allowed values of α are $25\text{--}85^\circ$ for norbornene, $45\text{--}60^\circ$ for *cis*-stilbene, and 90° for *trans*-stilbene. None of the alkenes can approach the Fe–O bond in a perpendicular fashion suitable for interaction with both Fe and O to provide a metallaoxetane by a $2a + 2s$ cycloaddition.

a model catalyst in which the active site is encumbered by the bulky *o*-bromo substituents. The results of the epoxidation reactions are shown in Table I. Methods for product analysis have been described.^{3d,13} The stability and catalytic efficiency of $(\text{Br}_8\text{TPP})\text{Fe}^{\text{III}}(\text{Cl})$ is shown by the 92% yield of the TME epoxide without porphyrin decomposition (determined by the comparison

(9) The Br_8TPPH_2 was prepared from 2,6-dibromobenzaldehyde [mp $90\text{--}91^\circ\text{C}$, (lit.¹⁰ 90.5°C)] and coarsely purified according to the procedure by Lindsey.¹¹ Iron insertion was performed in refluxing DMF/toluene = 4:1 (24 h) using a 100-fold excess of anhydrous FeCl_2 . The product was purified by chromatography on acidic (HCl) alumina with CH_2Cl_2 as the eluent: ^1H NMR (CD_2Cl_2) δ 80.7 s (8 H, pyrrole H), 13.6 s (4 H, Ph *m*-H), 12.5 s (4 H, Ph *m*-H), 8.2 s (4 H, Ph *p*-H); mass spectrum (laser desorption;¹² calcd for $\text{C}_{44}\text{H}_{20}\text{N}_4\text{Br}_8\text{FeCl}$, MW = 1335.20; obsd, m/e 1335 (M^+), 1300 ($\text{M}^+ - \text{Cl}$) (clusters of peaks due to Br isotope distribution).

(10) Lock, G. *Ber.* **1935**, 68B, 1505.

(11) Lindsey, J. S.; Schreiman, I. C.; Hsu, H. C.; Kerney, P. C.; Marguerettaz, A. M. *J. Org. Chem.* **1987**, 52, 827.

(12) Mass spectral analysis was performed by Prof. Charles L. Wilkins at the Department of Chemistry, University of California, Riverside.

(13) Dicken, C. M.; Lu, F.-l.; Nee, M. W.; Bruice, T. C. *J. Am. Chem. Soc.* **1985**, 107, 5776.

(14) Hoard, J. L.; Cohen, G. H.; Glick, M. D. *J. Am. Chem. Soc.* **1967**, 89, 1992.

(15) Penner-Hahn, J. E.; Smith Eble, K.; McMurry, T. J.; Renner, M.; Balch, A. L.; Groves, J. T.; Dawson, J. H.; Hodgson, K. O. *J. Am. Chem. Soc.* **1986**, 108, 7819.

(4) Sawyer, D. T. *J. Am. Chem. Soc.* **1988**, 110, 2465.

(5) Groves, J. T.; Nemo, T. E. *J. Am. Chem. Soc.* **1983**, 105, 5786.

(6) Loew, G. H.; Kert, C. J.; Hjelmeland, L. M.; Kirchner, R. F. *J. Am. Chem. Soc.* **1977**, 99, 3534.

(7) Groves, J. T.; Nemo, T. E. *J. Am. Chem. Soc.* **1983**, 105, 6243.

(8) Streitwieser, A., Jr.; Owens, P. H. *Orbital and Electron Density Diagrams: An Application of Computer Graphics*; The Macmillan Company: New York, 1973.

of UV-vis spectra before and at the completion of reaction) at a catalyst turnover number of 200, $[(\text{Br}_8\text{TTP})\text{Fe}^{\text{III}}(\text{Cl})] = 4.5 \times 10^{-5} \text{ M}$, $\text{C}_6\text{F}_5\text{IO}$ to TME is 1.0:1.1.

Computer graphics show that alkenes can approach the iron bound oxygen only from the top (Figure 1). TME requires a large value of α (I), while smaller values of α suffice for norbornene and *cis*-stilbene. Clean epoxidation of *cis*-stilbene (the substrate prone to rearrangements^{3d}) indicates that the distances between the double bond and the orbitals on iron or porphyrin nitrogen are too large for the interactions which would lead to rearrangement products^{3d} and that the only interaction possible is that between the alkene orbitals and orbitals on iron bound oxygen. Thus, the only interaction required for epoxidation is between the alkene double bond and oxygen.^{3d} Due to severe steric hindrance *trans*-stilbene virtually does not epoxidize at all.

Taken alone, the requirement for alkene to approach the iron bound oxygen with a modest value of α allows several mechanisms. These are as follows: (i) direct oxene insertion into the alkene double bond; (ii) initial $1e^-$ oxidation of the alkene followed by collapse of the alkene π -cation radical and iron(IV)-oxo porphyrin to epoxide plus iron(III) porphyrin; and (iii) formation of a $\text{Fe}^{\text{IV}}\text{-O-C-C}^+$ transient species which gives way to epoxide plus iron(III) porphyrin. Disfavored are mechanisms requiring the approach of alkene to iron(IV)-oxo porphyrin π -cation radical from the side and with small values of α and the obligatory formation of a metallaoxetane (see figure legend).

Acknowledgment. This work was supported by grants from the National Institutes of Health and the National Science Foundation.

Photo-Arbusov Rearrangements of Benzyl Phosphites

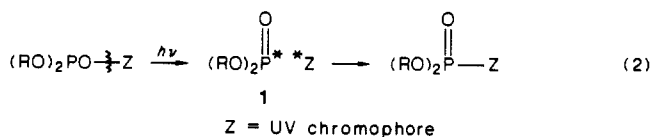
Jan Omelanzcuk, Alan E. Sopchik, Sueg-Geun Lee, Kunihiro Akutagawa, S. Matthew Cairns, and Wesley G. Bentrude*

Department of Chemistry, University of Utah
Salt Lake City, Utah 84112
Received June 10, 1988

The *thermal* Arbuzov rearrangement is a widely known¹ reaction of organophosphorus molecules, eq 1. It classically occurs via a two-step mechanism catalyzed by R-X ($\text{X} = \text{halide, tosylate, etc.}$) and in certain instances can be autocatalytic.^{1c} Intermolecular free-radical Arbuzov reactions are known as well.²

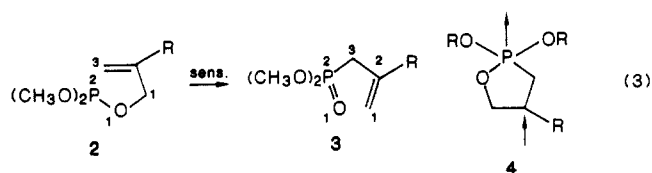


It seemed to us possible that absorption of UV light could result in reaction 2, a *photochemical* Arbuzov rearrangement.⁴ With

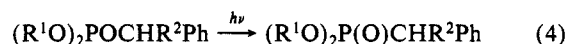


a sufficiently weak O-Z bond, useful regioselectivity might result. Radical or ion-pair intermediates (1) potentially could be pro-

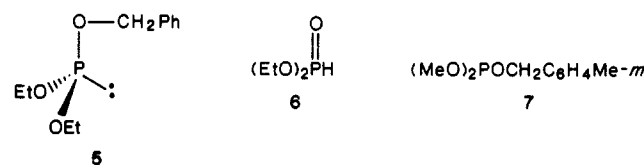
duced. We showed recently that under conditions of triplet sensitization allyl phosphites, **2**, are photorearranged in an *intramolecular* Arbuzov-like process which is formally a cyclic 2,3-sigmatropic rearrangement, $2 \rightarrow 3$, eq 3.⁵ A cyclic triplet phosphoranyl 1,3-biradical (**4**) was suggested as a likely intermediate.



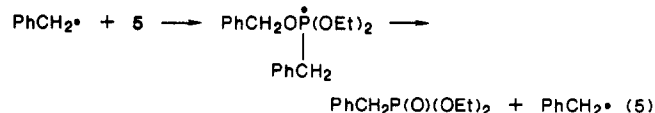
We report here the photorearrangement of benzyl dialkyl phosphites to the corresponding dialkyl benzylphosphonates, reaction 4. The specific processes examined are clean, regioselective, and largely intramolecular. The rearrangements occur with a variety of benzylic phosphites to give potentially useful phosphonates.



Irradiations of 0.1–0.2 M solutions of phosphite **5** in deoxygenated benzene in quartz tubes (450-W medium pressure Hg lamp) gave $\text{PhCH}_2\text{P}(\text{O})(\text{OEt})_2$ in 85–95% yield at 90–100% conversion (^{31}P NMR, ^1H coupled; or ^1H NMR). Evidence for free-radical formation was found in the GLC detection, at nearly complete consumption of **5**, of 0.5–1% of bibenzyl (equivalent to

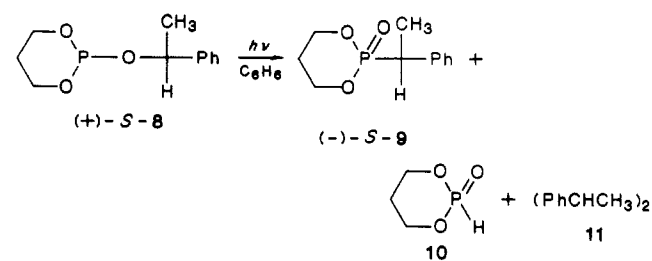


1–2% of cage-free $\text{PhCH}_2\cdot$) and 0.5–1% of phosphite **6**. Irradiation of a 1:1 mixture of **5** and **7** in benzene gave only minor amounts (1–2%) of the crossover phosphonates (^{31}P NMR). Chain reaction sequence 5 or more than minor reaction via combination of *cage-free* radical pairs is thereby excluded.



Reaction 2 ($\text{Z}^* = \text{PhCH}_2^+$, $\text{R} = \text{Et}$) gives a reasonable interpretation of these results. Initial radical pair **1** is short-lived and undergoes very predominantly *cage recombination* to product benzylphosphonate, i.e., $k_{\text{comb}} \gg k_{\text{diff}}$. Cage-free radicals in minor amounts also recombine to form $(\text{EtO})_2\text{P}(\text{O})\text{CH}_2\text{Ph}$ and bibenzyl. (The possible formation of the dimer of $(\text{EtO})_2\text{P}(\text{O})\cdot$ has not been investigated.) Added MeOH failed to produce so much as 1% of MeOCH_2Ph or any toluene, the trapping products of diffusive separation of PhCH_2^+ or $\text{PhCH}_2\cdot$ from potential ion-pair intermediate **1**.

The rearrangement of **8** in C_6H_6 proceeds in 84–92% yield (GLC) at 72–98% conversion with *close to complete retention of configuration of stereochemistry at the chiral carbon* ($8 \rightarrow 9$). Dimer **11**, 0.2–1% yield, also is seen by GLC. Again k_{comb}



(1) (a) Bhattacharya, A. K.; Thyagarajan, G. *Chem. Rev.* **1981**, *81*, 415. (b) Brill, T. S.; Landon, S. J. *Ibid.* **1984**, *84*, 577. (c) Lewis, E. S.; Hamp, D. J. *Org. Chem.* **1983**, *48*, 2025.

(2) (a) Bentrude, W. G.; Alley, W. D.; Johnson, N. A.; Murakami, M.; Nishikida, K.; Tan, H. W. *J. Am. Chem. Soc.* **1977**, *99*, 4383. (b) For references to other radical Arbuzovs, see: Bentrude, W. G. *Acc. Chem. Res.* **1982**, *15*, 117. Davies, A. G.; Griller, D.; Roberts, B. P. *J. Chem. Soc., Perkin Trans 2* **1972**, 2224. Bentrude, W. G.; Fu, J. J. L.; Rogers, P. E. *J. Am. Chem. Soc.* **1973**, *95*, 3625 and references therein.

(3) Mark, V. *Mech. Mol. Mgr.* **1969**, *2*, 319 and ref given in ref 1a and 1b. Fu, J. J. L.; Bentrude, W. G. *J. Am. Chem. Soc.* **1972**, *94*, 7710.

(4) Trialkyl phosphites undergo photo-Arbuzov rearrangements under the conditions of this report extremely slowly if at all. (See, however: LaCount, R. B.; Griffin, C. E. *Tetrahedron Lett.* **1965**, 3071).

(5) Bentrude, W. G.; Lee, S. G.; Akutagawa, K.; Ye, W.; Charbonnel, Y. *J. Am. Chem. Soc.* **1987**, *109*, 1577.